YMTHE, Volume *27*

Supplemental Information

Combined Antitumor Effects of Sorafenib and GPC3-CAR T Cells in Mouse Models of Hepatocellular Carcinoma

Xiuqi Wu, Hong Luo, Bizhi Shi, Shengmeng Di, Ruixin Sun, Jingwen Su, Ying Liu, Hua Li, Hua Jiang, and Zonghai Li

Supplemental Figures

Supplementary Figure S1:

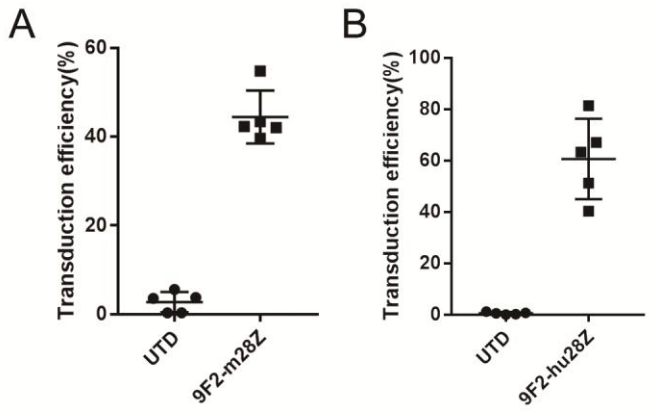

Supplementary Figure S1: Transduction efficiencies of murine and human CAR T cells. (A) Mouse T cells were transduced by 9F2-m28Z with positive rate as 45% on average. (B) Human T cells were transduced by 9F2-hu28Z with positive rate as 60% on average. The results are expressed as the mean ± SEM.

Supplementary Figure S2:

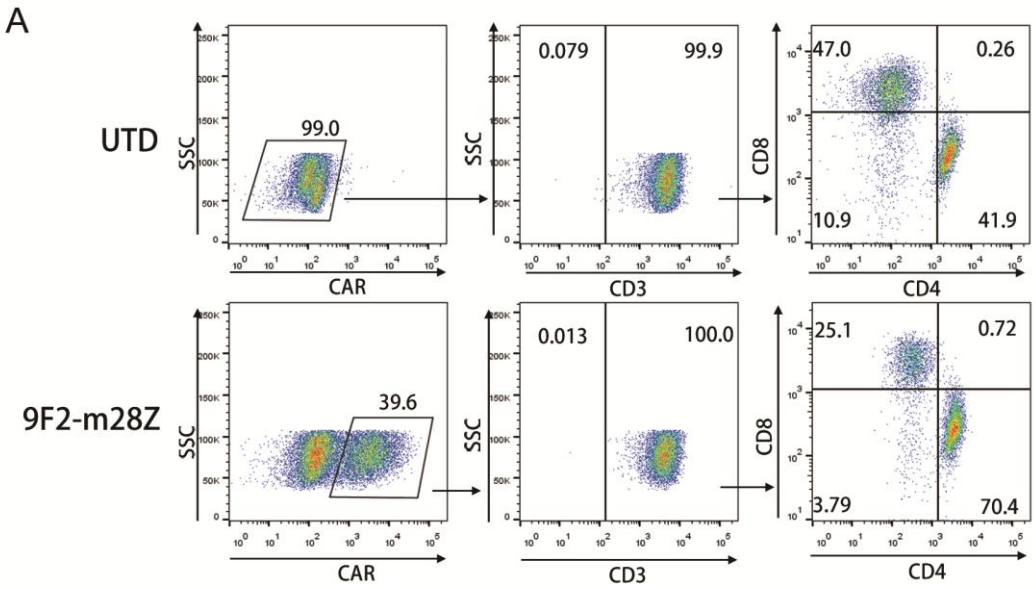

Supplementary Figure S2: Basic phenotypes of murine CAR T cells. (A) A representative flow cytometry analysis of CD3, CD4, CD8 expression on untransduced (UTD) mouse T cells and mCAR T cells transduced with 9F2-m28Z.

Supplementary Figure S3:

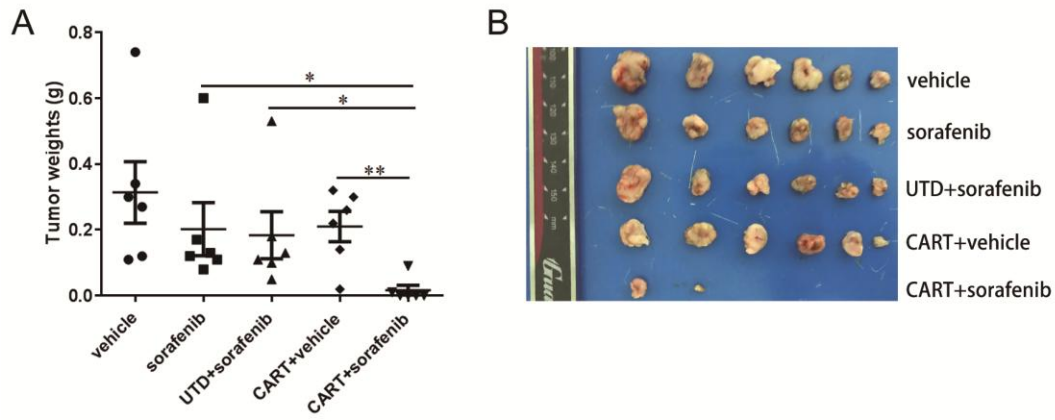

Supplementary Figure S3: Tumor samples after sorafenib and CAR T cell treatment. On day 28 after the last determination, mice were euthanized. Then, tumor weight was measured (A) and tumor samples were exhibited in (B). The results are expressed as the mean ± SEM. Significance of findings was defined as follows: ns, not significant; $p > 0.05$; *$p < 0.05$; **$p < 0.01$; or ***$p < 0.001$.

Supplementary Figure S4:

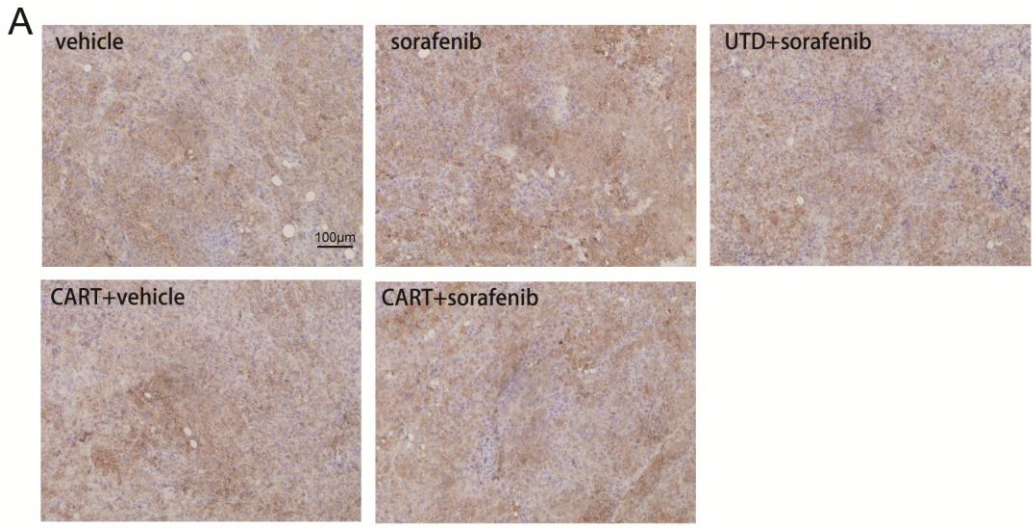

Supplementary Figure S4: chGPC3 expression within tumor samples after sorafenib and CAR T cell treatment. (A) Representative immunostaining images of chGPC3 expression in tumor tissues. Scale bars, 100μM.

Supplementary Figure S5:

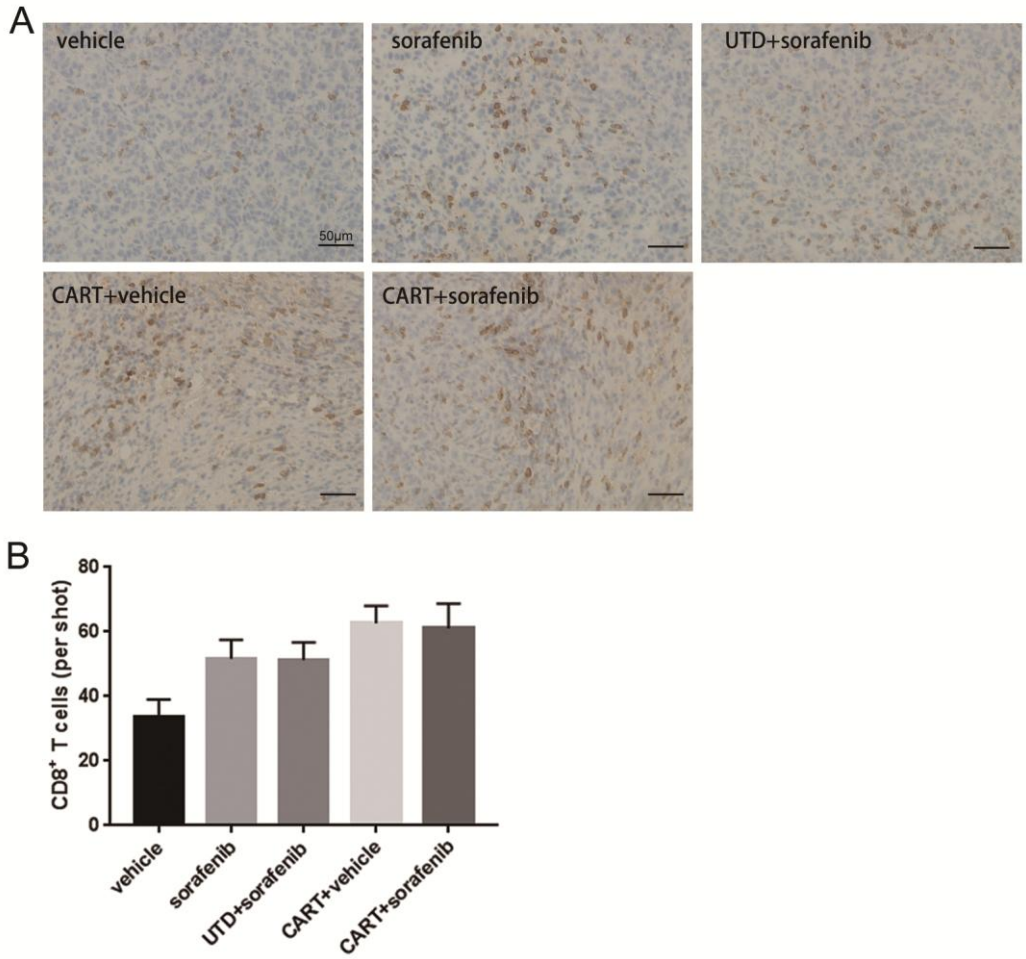

Supplementary Figure S5: Representative images of CD8+ mouse T cell infiltration in tumor tissues. (A) Representative images of $CD8^+$ mouse T cell infiltration in tumor tissues as detected by immunohistochemistry staining. Scale bars, 50μM. (B) Quantification of $CD8^+$ mouse T cell infiltration in tumor tissues (n=5). The results are expressed as the mean ± SEM.

Supplementary Figure S6:

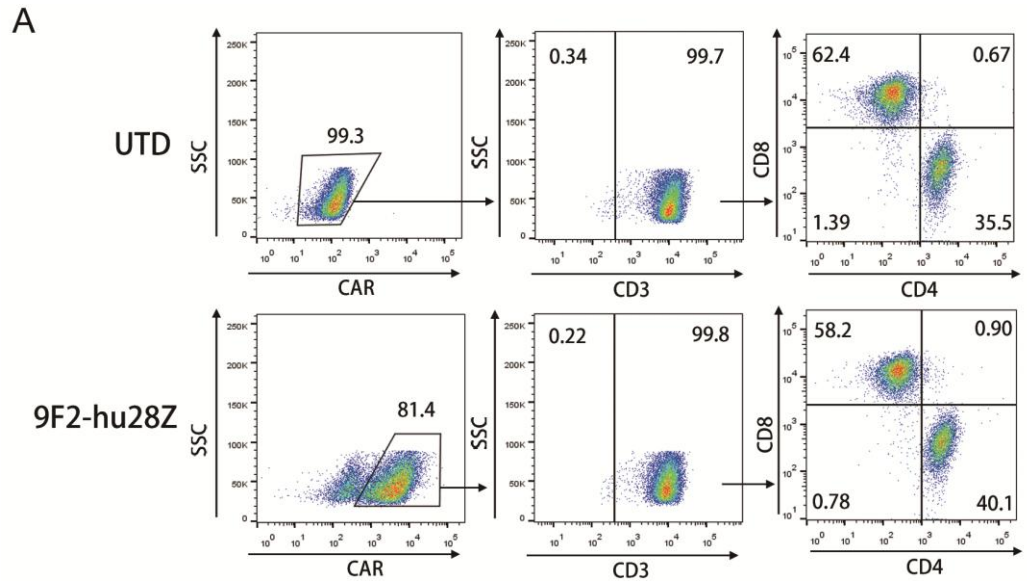

Supplementary Figure S6: Basic phenotypes of human CAR T cells. (A) A representative flow cytometry analysis of CD3, CD4, CD8 expression on untransduced (UTD) human T cells and huCAR T cells transduced with 9F2-hu28Z.

Supplementary Figure S7:

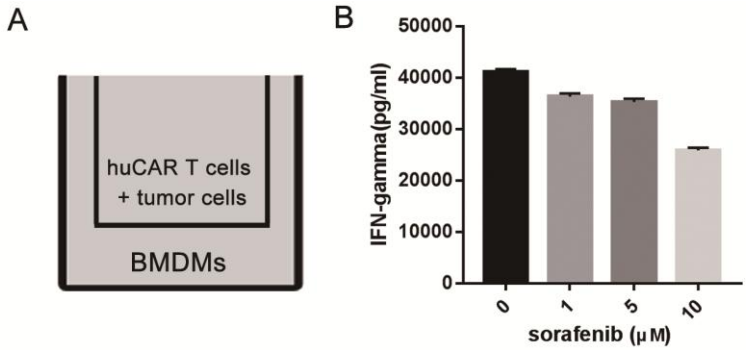

Supplementary Figure S7: Sorafenib-treated BMDMs did not enhance the function of huCAR T cells in vitro. (A and B) Transwell co-culture of huCAR T cells with BMDMs. BMDMs were treated with sorafenib and LPS (10 ng/mL) for 8 hours. Then huCAR T cells and tumor cells were added into the upper chamber for another 16h co-culture with sorafenib-treated BMDMs. IFN-γ expression in supernatants were assayed by cytometric bead array (CBA). Data reflects mean ± SD of triplicate wells.

Supplementary Figure S8:

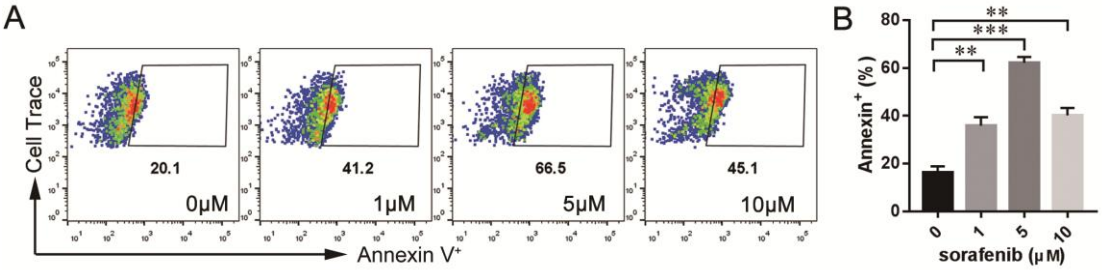

Supplementary Figure S8: Apoptosis of Hepa1-6-chGPC3 cells was significantly increased when mCAR T cells were combined with sorafenib. (A and B) Representative flow cytometry plots and quantification results showing the frequencies of Annexin V^+ Hepa1-6-chGPC3 cells after sorafenib and mCAR T cells treatment. Before Annexin V Staining, Hepa1-6-chGPC3 cells were pre-labeled with Cell Trace Violet dye and then treated with mCAR T cells at 1: 10 ratio and various concentrations of sorafenib for 24h. Results are expressed as mean ± SEM of triplicates. Significance of findings was defined as follows: ns, not significant; $p > 0.05$; *$p < 0.05$; **$p < 0.01$; or ***$p < 0.001$.